Title
Calmodulin Promotes N-BAR Domain-Mediated Membrane Constriction and Endocytosis

Journal
Developmental Cell, 37(2)

ISSN
1534-5807

Authors
Myers, Margaret D
Ryazantsev, Sergey
Hicke, Linda
et al.

Publication Date
2016-04-01

DOI
10.1016/j.devcel.2016.03.012

Peer reviewed

HHS Public Access

Author manuscript

Dev Cell. Author manuscript; available in PMC 2017 April 18.

Published in final edited form as:

Dev Cell. 2016 April 18; 37(2): 162–173. doi:10.1016/j.devcel.2016.03.012.

Calmodulin promotes N-BAR domain-mediated membrane constriction and endocytosis

Margaret D. Myers[1], **Sergey Ryazantsev**[1], **Linda Hicke**[2], and **Gregory S. Payne**[1,*]

[1]Department of Biological Chemistry, David Geffen School of Medicine, University of California Los Angeles, Los Angeles, CA, 90095, U.S.A

[2]Molecular Genetics and Microbiology, College of Natural Sciences, University of Texas at Austin, Austin, Texas, 78712, U.S.A.

SUMMARY

Membrane remodeling by BAR (Bin, Amphiphysin, RVS) domain-containing proteins, such as endophilins and amphiphysins, is integral to the process of endocytosis. However, little is known about regulation of endocytic BAR domain activity. We have identified an interaction between the yeast Rvs167 N-BAR domain and calmodulin. Calmodulin-binding mutants of Rvs167 exhibited defects in endocytic vesicle release. In vitro, calmodulin enhanced membrane tubulation and constriction by wild-type Rvs167 but not calmodulin binding-defective mutants. A subset of mammalian N-BAR domains bound calmodulin, and coexpression of calmodulin with endophilin A2 potentiated tubulation *in vivo*. These studies reveal a conserved role for calmodulin in regulating the intrinsic membrane sculpting activity of endocytic N-BAR domains.

Abstract

*Correspondence: gpayne@mednet.ucla.edu, telephone: (310) 206-3121, fax: (310) 206-1929.

AUTHOR CONTRIBUTIONS

Conceptualization, M.M., G.P. and L.H.; Methodology, M.M. and G.P.; Formal Analysis, M.M.; Investigation, M.M. and S.R.; Resources, G.P.; Writing – Original Draft, M.M.; Writing – Review & Editing, M.M. and G.P.; Visualization, M.M.; Supervision, G.P.; Funding Acquisition, M.M. and G.P.

eTOC:

Membrane remodeling by N-BAR domain-containing proteins is integral to the process of endocytosis. Myers et al. have identified a conserved interaction between endocytic N-BAR domains and calmodulin. The authors find that calmodulin regulates the intrinsic membrane sculpting activity of the N-BAR domain and is required for endocytosis in yeast.

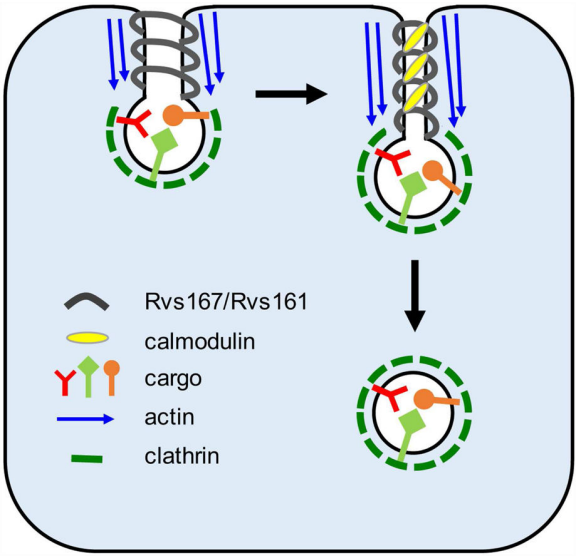

INTRODUCTION

Clathrin-coated vesicle (CCV)-mediated endocytosis plays a fundamental role in cellular processes including nutrient uptake, receptor signaling and down-regulation, synaptic vesicle recycling, and plasma membrane remodeling. The clathrin coat that drives vesicle formation is assembled from three main types of evolutionarily conserved proteins: clathrin, which assembles into an outer scaffold; clathrin adaptors, which couple clathrin to the plasma membrane and cargo; and a variety of endocytic accessory factors, which contribute a broad spectrum of functions critical to vesicle formation.

One class of endocytic accessory proteins is defined by BAR domains (Frost et al., 2009; Mim and Unger, 2012; Rao and Haucke, 2011). BAR domains dimerize to form crescent-shaped structures that can induce and/or stabilize membrane curvature. Through these activities, BAR domain proteins play key roles in the membrane sculpting required during vesicle invagination, constriction, and scission (Daumke et al., 2014; Qualmann et al., 2011; Ren et al., 2006). A subset of BAR domains, termed N-BAR domains, contain an amphipathic helix N-terminal to the BAR domain that can insert into the lipid bilayer to promote membrane curvature. Accordingly, N-BAR proteins function mostly at the stage of vesicle neck constriction and scission, where the degree of membrane curvature is high.

In mammalian cells, N-BAR proteins endophilin and amphiphysin/BIN function in endocytic CCV formation (Daumke et al., 2014; Ren et al., 2006). This group of N-BAR proteins is complex, encoded by at least 5 endophilin genes and four amphiphysin/BIN genes, with multiple amphiphysin/BIN splice variants. In contrast, *Saccharomyces cerevisiae* expresses only two N-BAR proteins, Rvs161 and Rvs167. Rvs161 and Rvs167 associate through their N-BAR domains into heterodimers, and each is individually necessary for both fluid-phase and receptor-mediated endocytosis (Munn et al., 1995). Rvs167/161 are transiently recruited to nascent endocytic structures as the membrane becomes deeply invaginated, and the proteins depart concurrently with vesicle scission

(Kaksonen et al., 2005). Deletion of either *RVS161* or *RVS167* results in a distinctive defect: a proportion of invaginating coat structures retract back to the plasma membrane rather than progress through vesicle release (Kaksonen et al., 2005; Kishimoto et al., 2011). These findings have led to a model in which the yeast N-BAR proteins promote vesicle scission together with other components of the endocytic machinery.

Identifying mechanisms that control BAR domain activity is key to understanding how BAR domains mediate membrane remodeling in different cellular contexts. Several BAR domain regulatory mechanisms have been described including autoinhibition, interactions with small GTPases that mediate membrane targeting, and phosphoregulation of membrane binding and bending (Frost et al., 2009; Rao and Haucke, 2011). However, little is known about regulation of the N-BAR family of BAR domains. Here we report that calmodulin promotes membrane tubulation by binding to the N-BAR domains of yeast Rvs167 and a subset of mammalian endophilins and amphiphysins. These findings identify calmodulin binding as a conserved mechanism for regulation of BAR domain function *in vivo*.

RESULTS

The Rvs167 N-BAR domain binds calmodulin

Rvs167 contains an N-terminal N-BAR domain, a central region rich in glycine, proline, and alanine (GPA), and a C-terminal SH3 domain (Figure 1A) (Bauer et al., 1993). Domain analyses indicate that the BAR domain constitutes the key functional element in Rvs167 (Colwill et al., 1999; Sivadon et al., 1997). We used an Rvs167 fragment including the N-BAR domain (aa1-291) as bait in a yeast 2-hybrid screen for interacting proteins. One candidate interaction partner identified by the screen was calmodulin, which is required for endocytosis in yeast (Kubler et al., 1994). To independently test for interaction, lysates from bacteria expressing recombinant full-length or Rvs167 fragments (Figure 1A) were incubated with calmodulin-agarose or protein A sepharose as a negative control. Full-length Rvs167 and domain fragments containing the N-BAR domain specifically bound to calmodulin (Figure 1B). Similar results were obtained using purified recombinant Rvs167 forms, consistent with a direct interaction (Figure 1C). Rvs167 could be co-immunoprecipitated with epitope-tagged calmodulin from yeast cell lysates (Figure 1D), demonstrating that the interaction occurs *in vivo*. These results identify calmodulin as a binding partner of the Rvs167 N-BAR domain.

Calmodulin binding-defective mutants of Rvs167

To test the function of calmodulin binding *in vivo*, we sought to generate calmodulin binding mutants of Rvs167. Based on homology modeling, the Rvs167 N-BAR domain is predicted to contain an N-terminal amphipathic helix followed by three α-helices (Figure 2A) (Youn et al., 2010). The N-terminal helix/α-helix 1 and α-helix 2 independently interacted with calmodulin (Figure 2B). In the context of the full Rvs167 N-BAR domain, deletion of the N-terminal amphipathic helix substantially reduced calmodulin binding (Figure 2C), suggesting that this helix contains a calmodulin binding site. However, deletion of the N-terminal helix also reduced BAR domain binding to liposomes (Figure 2C). This result, and the established role of the amphipathic helices in membrane tubulation, potentially

complicates interpretation of the effects of mutations in this region. Therefore, we focused on defining the calmodulin binding site in α-helix 2.

Truncations of α-helix 2 (aa80-172) from either the N- or C-terminus were used to map calmodulin binding to the region between aa137 and aa161 (Figure S1A,B). Additionally, analysis of the Rvs167 sequence using the Calmodulin Target Database (http://calcium.uhnres.utoronto.ca/ctdb/ctdb/home.html) (Yap et al., 2000) revealed aa133-155 as a potential calmodulin binding region (Figure 2D). When alanine was substituted for hydrophobic residues in this sequence, calmodulin binding was reduced in every case but L154 (Figure 2E). Together, these results provide evidence that calmodulin interacts with sites in both the N-terminal amphipathic helix and α-helix 2 of the Rvs167 BAR domain, both of which are required for optimal calmodulin binding *in vitro*.

Of the mutations, L136A, I138A and I142A had minimal effects on liposome binding (Figure 2E). However, in a structural model of the Rvs167 N-BAR domain based on the crystal structure of the Drosophila amphiphysin BAR domain (PDB:1URU) (Berman et al., 2003), L136 is predicted to be part of the lipid-binding surface (Figure S1D). In contrast, I138 and I142 (and L135) are positioned on a surface distinct from sites predicted to interact with the membrane or Rvs161, while I139 lies mostly buried within the domain interior (Figure S1C,D).

Calmodulin binding by Rvs167 is important for endocytosis

I138A and I142A calmodulin-binding mutations were introduced into the endogenous *RVS167* locus and Cmd1 binding was assessed by co-immunoprecipitation using a functional GFP-tagged calmodulin. Compared to wild-type (WT) Rvs167, interaction of either mutant with calmodulin was significantly impaired (Figure 3A). In contrast, equivalent levels of Rvs161 were co-immunoprecipitated with all forms of Rvs167 (Figure 3B), suggesting that the mutations do not have a global effect on Rvs167 N-BAR domain structure.

Fluid-phase endocytosis was evaluated with Lucifer yellow (LY), a soluble fluorescent dye that is delivered via the endocytic pathway to the vacuole (Dulic et al., 1991). Vacuolar accumulation of LY was reduced in I138A and I142A mutant cells, compared to WT, although not to the extent observed for a full deletion of *RVS167* (Figure 3C,D). Consistent with a defect in endocytosis caused by decreased calmodulin binding to I138A and I142A mutants, overexpression of Cmd1 partially restored endocytosis in these mutants but not in cells lacking Rvs167 (Figures 3E and S2).

To assess endocytosis of a plasma membrane protein, we used Mup1-GFP (methionine transporter) expressed from the endogenous locus. In the absence of exogenous methionine, Mup1p accumulates at the cell surface (Figure 3F) (Menant et al., 2006). Addition of methionine triggers Mup1 internalization and transport to the vacuole. In WT cells, at 45 minutes after methionine addition, Mup1-GFP was no longer apparent at the plasma membrane and nearly 80% was quantified as internal (Figure 3F,G). In the calmodulin-binding mutants, a portion of Mup1-GFP was still visible at the plasma membrane and significantly less Mup1-GFP accumulated intracellularly, though more than that observed in

*rvs167*Δ cells (Figure 3F,G). The defects in internalization of LY and Mup1 caused by the I138A or I142A mutations provide evidence that calmodulin binding to Rvs167 promotes endocytosis.

Cells deficient in Rvs167 display a number of other phenotypes, including reduced viability upon starvation, slow growth on high salt concentrations, and temperature sensitivity (Ren et al., 2006). None of these phenotypes were reproducibly apparent in the calmodulin binding mutants, suggesting that calmodulin binding plays a specific role in endocytosis.

Live cell imaging of endocytic machinery components has delineated the spatio-temporal pattern of events that occur during formation of an endocytic vesicle (Kaksonen et al., 2005). Initially, clathrin and clathrin adaptor proteins are recruited to form a patch on the plasma membrane. Soon thereafter, other clathrin adaptors such as Sla1 as well as actin polymerization factors are recruited. Subsequent actin polymerization is accompanied by slow membrane invagination. Towards the end of this slow mobile phase, Rvs167/161 heterodimers are recruited to the neck of the forming invagination. Rvs167/161 recruitment is followed quickly by vesicle scission, uncoating, and fast movement of the vesicle into the cytoplasm.

Localization and dynamics of calmodulin at endocytic sites was examined by confocal microscopy of cells co-expressing calmodulin-GFP with 2xRFP-tagged Rvs167 or the actin binding protein Abp1-RFP as a reporter for actin filament assembly (Kaksonen et al., 2003). In both cases, substantial colocalization was observed (Figure 4A). The dynamics of calmodulin appearance and disappearance at patches matched that of Abp1 (Figure 4B). We were unable to directly compare calmodulin and Rvs167 dynamics because of low protein expression levels. However, Abp1 is recruited prior to Rvs167 (Figure 4B) and remains associated with the coat through the time that Rvs167 is present, implying the same relationship between calmodulin and Rvs167.

Cells lacking Rvs167 (or Rvs161) display a unique defect in endocytic patch dynamics: a fraction of the patches appear to retract to the plasma membrane rather than progressing to vesicle scission (Kaksonen et al., 2005; Kishimoto et al., 2011). This unusual phenotype has been interpreted as a failure to undergo scission. We used Sla1-GFP to monitor endocytic patch progression in WT and mutant cells. The I138A mutants exhibited an intermediate level of retractions compared to WT or *rvs167*Δ cells (Figure 4C,D). This result is consistent with the partial defects in LY and Mup1 endocytosis observed in I138A cells.

A role for calmodulin binding in Rvs167 localization at endocytic sites could account for the endocytic defects caused by the I138A mutation. However, recruitment of WT and I138A mutant Rvs167-GFP to patches were indistinguishable; no obvious differences were observed in the number and intensity of patches, and the lifetimes of mutant Rvs167-GFP at the patches were only slightly longer than WT (Figure 4E,F; WT = 9.44 ± 0.19s versus I138A = 10.59 ± 0.25s). Together our results suggest that calmodulin binding is not critical for Rvs167 localization at endocytic patches but instead likely contributes to Rvs167 tubulation activity prior to vesicle scission.

Endocytosis-defective calmodulin mutants are impaired in binding to Rvs167

Calmodulin is a well-characterized calcium binding protein that acts in both calcium-dependent and calcium-independent processes (Cyert, 2001). Binding of the Rvs167 N-BAR domain (1-265) to calmodulin-agarose or GST-calmodulin did not require addition of calcium, nor did additional calcium stimulate binding. However, binding was sensitive to the calcium chelator EGTA, an effect reversed by providing exogenous calcium (Figure 5A,B). These results indicate that calcium is required for calmodulin to associate with the Rvs167 N-BAR domain. Supporting this conclusion, Cmd1-3 and Cmd1-6, calmodulin mutants that cannot bind calcium due to mutations in all three EF hand motifs, were severely compromised for binding (Figure 5B).

Analyses of a collection of calmodulin mutants have provided evidence for distinct calmodulin functions in different cellular processes, including endocytosis (Ohya and Botstein, 1994a, b). In direct binding assays using mutant forms of GST-calmodulin, there was a strong correlation between mutations associated with endocytic phenotypes (F16A, F19A, F92A, F89A and F140A) and impaired binding to the Rvs167 N-BAR domain (Figure 5C). Reduced interactions are not due to defects in calcium binding by calmodulin, as none of the mutations altered calcium binding by gel mobility shift assays (Okano et al., 1998).

Our results indicate that calmodulin depends on calcium binding for interaction with Rvs167, and the Rvs167-calmodulin interaction is required for efficient endocytosis, suggesting that endocytosis should be dependent on calcium binding by calmodulin. Accordingly, LY uptake was evaluated in cells expressing the calcium-binding Cmd1-3 mutant. For comparison, we used cells expressing the temperature-sensitive *cmd1-1* allele, which functions normally at the permissive temperature of 24°C, but is defective for endocytosis at 37°C (Kubler et al., 1994). At 2 4°C, LY uptake was decreased in *cmd1-3* cells compared to *cmd1-1* cells (Figure 5D,E).

In addition to impaired calcium binding, the mutations present in *cmd1-3* (D20A, E31V, D56A, E67V, D93A, E104V) also confer temperature sensitivity (Geiser et al., 1991), raising the possibility that the endocytic defect observed in *cmd1-3* may not solely be due to loss of calcium binding. Therefore, we tested *cmd1-6*, a mutant form of calmodulin that cannot bind calcium but is not temperature sensitive (D20A, D56A, D93A). LY endocytosis was impaired in cells expressing Cmd1-6 (Figure S3A), indicating that the defect in endocytosis can be attributed to loss of calcium binding, not to other effects caused by mutations in *cmd1-3*.

Our findings contrast with a previous study reporting that receptor-mediated α-factor pheromone internalization, which requires both calmodulin and Rvs167, proceeds normally in cells expressing Cmd1-3, suggesting that calmodulin does not require high affinity calcium binding to function in endocytosis (Kubler et al., 1994). In the previous study, pheromone was pre-bound to *cmd1-3* cells on ice before shifting the cells to 24°C. In contrast, our LY assays were carried out at a constant temperature (24°C). This difference in methodology suggested that a temperature shift might compensate for defective *cmd1-3* activity. Indeed, preincubation of *cmd1-3* cells on ice stimulated LY uptake into *cmd1-3*

cells (Figure S3B,C). Notably, there is precedent for temperature shift-induced rescue of endocytic defects in mammalian cells (Miller et al., 2015). By another constant temperature assay, *cmd1-3* cells are also less sensitive than WT cells to K28 killer toxin, which requires endocytosis for toxicity (Carroll et al., 2009) (Figure S3D). Taken together, these data provide evidence that calcium binding plays a previously unappreciated role in the endocytic function of calmodulin, consistent with the calcium-sensitive binding of calmodulin to other known endocytic targets (Geli et al., 1998; Schaerer-Brodbeck and Riezman, 2000).

To probe potential sources of calcium in endocytosis, LY uptake was assessed in cells under calcium-free or calcium-replete conditions (Figure S3E). Levels of internalized LY were equivalent under both conditions, indicating that extracellular calcium is not required for endocytosis. In contrast, LY uptake was compromised in cells pre-incubated in BAPTA (Figure S3F), a cell-impermeant calcium chelator shown to deplete intracellular calcium (Bonilla et al., 2002). Exogenous calcium added simultaneously with BAPTA partially rescued the LY uptake defect, suggesting that the effect on LY uptake was due in part to calcium depletion. These data are consistent with an endocytic role for calcium from intracellular stores.

Calmodulin potentiates Rvs167-mediated membrane tubulation

We examined whether calmodulin affects N-BAR domain-mediated membrane binding and tubulation *in vitro*. Because Rvs167 functions with Rvs161 as a heterodimer *in vivo* (Friesen et al., 2006; Youn et al., 2010), we used extracts from bacteria coexpressing Rvs167 1-265 (which expresses at higher levels than full length Rvs167) and full-length Rvs161. GST-tagged calmodulin did not affect Rvs167/161 or I138A/Rvs161 binding to synthetic liposomes (Figure 6A). However, substantially more GST-calmodulin associated with liposomes in the presence of WT Rvs167/161 compared to I138A/161, indicating that the α-helix 2 binding site is important for calmodulin binding in the context of the membrane-associated heterodimer. In binding assays, increasing the levels of GST-calmodulin incubated with WT Rvs167/161 liposomes resulted in a molar ratio estimated at one calmodulin to four heterodimers. This ratio is likely an underestimate because saturation was not reached due to increased non-specific binding of GST-calmodulin to liposomes at high concentrations of calmodulin (Figure S4A).

To assess the role of calmodulin binding in Rvs167/161-mediated membrane tubulation, synthetic liposomes incubated with Rvs167/161 dimers in the presence or absence of calmodulin (Figure S4B) were examined by electron microscopy. Both Rvs167/161 and I138A/Rvs161 induced membrane tubules of comparable length and diameter in the absence of calmodulin (Figure 6B-D), demonstrating that the I138A mutation does not alter the intrinsic tubulation activity of Rvs167. The diameters of tubules generated by Rvs167/161 were similar to those previously observed for tubules produced by other N-BAR proteins (Mim et al., 2012; Wu et al., 2014a).

When incubated with liposomes, calmodulin alone did not produce tubules (Figure S4C). However, addition of calmodulin to Rvs167/161 resulted in a 25% increase in the average length of tubules, accompanied by a 14% decrease in tubule diameter (Figures 6B-D and S4D,E). In contrast, addition of calmodulin did not alter tubules formed by I138A/Rvs161.

Changes in tubule morphology were not observed when the calcium-binding mutant Cmd1-6 was combined with Rvs167/161, providing additional evidence that calcium is required for functional interaction between Rvs167 and calmodulin.

Physical and functional interaction of calmodulin with a subset of mammalian N-BAR domains

Calmodulin was tested for interaction with mammalian N-BAR proteins amphiphysin, Bin1 and endophilins A1, A2, B1 and B2. All but endophilins B1 and B2 exhibited some degree of binding to calmodulin-agarose (Figure 7A). Calmodulin associated with the N-BAR domains of amphiphysin and BIN1 (Figure 7B), not the C-terminal fragments. Similarly, calmodulin bound the N-BAR domains of endophilin A1 and A2. In these cases the C-terminal regions could not be analyzed because of low expression. Calmodulin binding to the N-BAR domains was generally elevated compared to the full-length proteins, perhaps due to autoinhibitory mechanisms similar to those described for certain other BAR domains (Rao et al., 2010; Vazquez et al., 2013; Zaidel-Bar et al., 2010).

The effect of calmodulin on mammalian N-BAR domain tubulation activity was examined by expressing GFP-tagged endophilin A2 BAR domain with either mCherry-tagged calmodulin or mCherry alone in COS-7 cells. In transfected cells, endophilin A2-GFP formed tubular structures that often emanated from the plasma membrane as determined by labeling the membrane with FM4-64 (Figure S5). Co-expression of calmodulin-mCherry with endophilin A2-GFP resulted in a lengthening of the tubules compared with mCherry alone, leading to an increase in the proportion of cells exhibiting longer tubules (Figure 7C,D). Although most of the calmodulin-mCherry was diffusely localized, examples of tubules labeled with both endophilin A2 BAR-GFP and calmodulin-mCherry were apparent. In contrast, co-expressed calmodulin had no effect on tubulation by endophilin B2 (Figure 7C,D), which did not interact with calmodulin *in vitro* (Figure 7A). Thus, similar to our results with Rvs167, calmodulin can bind specific mammalian N-BAR domains *in vitro* and potentiate N-BAR domain-mediated tubulation *in vivo*.

DISCUSSION

BAR domain proteins function in a variety of processes involving dynamic membrane shape changes within eukaryotic cells, yet relatively little is known about regulation of BAR domain activity. Our studies reveal an interaction between the N-BAR domain of yeast Rvs167 and calmodulin that potentiates endocytic vesicle release *in vivo* and membrane tubulation and tubule constriction *in vitro*. Calmodulin also binds to and stimulates tubulation by a subset of mammalian N-BAR domain proteins. These findings provide evidence that calmodulin binding serves as a conserved mechanism to augment the intrinsic membrane sculpting activity of specific N-BAR domains.

BAR domain dimers oligomerize into a helical assembly that shapes the underlying membrane into a tubule (Frost et al., 2008; Mim et al., 2012; Mizuno et al., 2010; Shimada et al., 2007). During endocytosis, this activity is thought to help constrict the neck of an invaginating vesicle and contribute to vesicle fission together with actin polymerization and changes in phosphoinositide levels (Kishimoto et al., 2011). Cryo-electron microscopic

reconstructions of membrane-bound endophilin N-BAR domains have provided a molecular model for the oligomeric state associated with membrane bending (Mim et al., 2012). The studies revealed a helical arrangement of N-BAR domains held together by low-affinity interactions between N-terminal amphipathic helices in adjacent rows. In the context of this model, our results suggest that calmodulin binding augments Rvs167 N-BAR domain function in the vesicle scission process by stimulating the assembly and/or stability of the membrane-associated N-BAR oligomeric helix in a way that constricts the helix diameter. At the near equal stoichiometry of calmodulin to Rvs167 that we observed by liposome binding assays, calmodulin could stimulate constriction by cross-linking adjacent Rvs167 BAR domains in the helix or by forming a cross-bridge between BAR domains in consecutive helix turns. Alternatively, considering that calmodulin contacts two distinct sites on the Rvs167 N-BAR domain including the N-terminal amphipathic helix, calmodulin binding within a single BAR domain could alter the conformation to favor oligomerization and constriction, as well as shift the membrane interaction of the N-terminal amphipathic helix membrane to destabilize the lipid bilayer. Preliminary studies of the calmodulin binding site within the Rvs167 N-terminal amphipathic helix indicate that calmodulin binds to residues in the helix that are predicted to face away from the membrane, suggesting it may be possible for the amphipathic helix to bind to calmodulin and lipids simultaneously. In any of these arrangements, calmodulin would likely assume an extended conformation similar to that described in cases where the two lobes of calmodulin bind to separate target sites (Drum et al., 2002; Liu et al., 2012; Schumacher et al., 2001). Consistent with this model, we observed that BAR domain interaction with calmodulin was diminished by single mutations in either calmodulin lobe that define distinct binding sites for calmodulin target proteins (Geli et al., 1998; Schaerer-Brodbeck and Riezman, 2000).

There are now three known calmodulin targets in the yeast endocytic machinery, Rvs167, Arc35, and Myo5, that can account for the calmodulin requirement in endocytosis (Geli et al., 1998; Schaerer-Brodbeck and Riezman, 2000). Each acts at relatively late stages in endocytosis: Arc35 as part of the Arp2/3 complex in actin filament assembly, Myo5 in actin filament assembly and actin-dependent membrane invagination, and Rvs167 during membrane invagination and constriction (Jonsdottir and Li, 2004; Kaksonen et al., 2005; Schaerer-Brodbeck and Riezman, 2000; Sun et al., 2006). The timing of calmodulin recruitment to endocytic patches that we observed in live cells is fully consistent with the dynamics of its binding partners. Calmodulin appeared at endocytic sites coincident with actin-binding Abp1, which is recruited at the same time as Arp2/3 (Kaksonen et al., 2003), and persists through the time of Rvs167 assembly and vesicle release. Calmodulin binding to Arc35 is required for calmodulin localization at endocytic sites, providing a basis for the timing of calmodulin recruitment (Schaerer-Brodbeck and Riezman, 2000). Whether calmodulin regulates Arp2/3 activity is unknown. In the case of Myo5, calmodulin serves to stabilize an autoinhibited state so that calmodulin must be discharged to trigger Myo5 activity (Grotsch et al., 2010). The basis for calmodulin release from Myo5 has not been defined, but it is intriguing that Rvs167 begins to assemble at endocytic sites immediately after Myo5 is recruited. This raises the possibility that calmodulin is transferred from Myo5 to Rvs167, providing a mechanism to temporally couple stimulation of actin-based invagination and N-BAR domain-mediated tubulation at the forming vesicle neck.

Our results indicate that Rvs167 binding to calmodulin depends on calcium. Calcium is also required for binding of Arc35 to calmodulin and stimulates the release of calmodulin from Myo5 (Geli et al., 1998; Grotsch et al., 2010; Schaerer-Brodbeck and Riezman, 2000). Thus, calmodulin interaction with all known targets in the yeast endocytic apparatus is sensitive to calcium. However, the *cmd1-3* mutant was reported to sustain WT levels of receptor-mediated pheromone endocytosis, leading to the conclusion that calmodulin function in endocytosis is independent of calcium binding (Kubler et al., 1994). In re-evaluating this paradox, we observed that *cmd1-3* cells exhibited partial defects in fluid-phase uptake of Lucifer yellow and resistance to killing by K28 killer toxin, which is dependent on receptor-mediated endocytosis (Carroll et al., 2009). The difference between our findings and those reported previously remains to be fully defined. It is worth noting however, that subjecting cells to the same temperature shift used in the pheromone uptake assay resulted in higher levels of Lucifer yellow uptake by *cmd1-3* cells, suggesting that temperature manipulation could be a factor. Supporting this view, when a constant-temperature pheromone uptake assay was used, overexpression of Cmd1-3 was less effective than overexpression of WT calmodulin in suppressing the endocytic defects of *arc35-1* cells (Schaerer-Brodbeck and Riezman, 2000). Taken together, these results provide evidence that calcium binding facilitates, but is not required for, calmodulin function in endocytosis. Initial experiments suggest that intracellular stores of calcium contribute endocytic activity, however the source and the relative contributions of calcium flux and resting calcium levels to calmodulin function during endocytosis await further investigation.

Calmodulin interacted with the N-BAR domains of a subset of mammalian proteins that we tested, including the endocytic proteins amphiphysin and endophilin A. Furthermore, cotransfection of calmodulin stimulated membrane tubulation by endophilin A2 in COS-7 cells. These findings provide evidence that the role of calmodulin as a stimulatory factor for N-BAR domain-mediated membrane bending has been conserved in mammals. Calmodulin has been functionally associated with endocytic processes in mammalian cell types such as chromaffin cells, neurons, and B lymphocytes that undergo large cytoplasmic calcium flux in response to external cues (Artalejo et al., 1996; Salisbury et al., 1980; Wu et al., 2009; Wu et al., 2014b; Yamashita et al., 2010; Yao and Sakaba, 2012). Our observation that calmodulin was able to stimulate endophilin-mediated tubulation in COS-7 cells raises a possibility that these types of large-scale regulated calcium fluxes may not be essential for this calmodulin activity. Thus, the conserved BAR domain regulatory mechanism that we describe here for calmodulin has the potential to apply to membrane bending events in a broader range of mammalian cell types.

EXPERIMENTAL PROCEDURES

Plasmids

Recombinant tagged and mutant forms of Rvs167, mammalian N-BAR proteins, and calmodulin were generated in pET30 (N-BAR proteins; Novagen) or pGEX-6P-2 (calmodulin; GE Healthcare) using standard methods (Supplemental Experimental Procedures). Point mutations were generated by site directed mutagenesis (Landt et al., 1990). Rvs167 (1-265) was co-expressed with Rvs161 from a bicistronic pET30 expression

vector. GFP-tagged endophilins A2 and B2 were expressed from pEGFP-N1 (Clontech). Mouse calmodulin tagged with mCherry was constructed in pmCherry-N1 (Clontech). For calmodulin overexpression experiments, *CMD1* was inserted into multicopy vector pRS426. All inserts were verified by DNA sequencing.

Yeast strains

Yeast strains used in this study are shown in the Supplemental Experimental Procedures. Cells were grown in standard media and all mutations and tags were introduced into endogenous loci by homologous recombination methods (Supplemental Experimental Procedures).

Calmodulin Binding Assays

Calmodulin binding assays were performed using either calmodulin coupled to Sepharose CL-4B (Stratagene) or GST-Cmd1 immobilized on glutathione-sepharose. Purified Rvs167/mammalian N-BAR domain proteins or lysates containing N-BAR domains/fragments of interest were incubated with calmodulin-agarose in the presence of 2 mM $CaCl_2$ (unless otherwise indicated) for 45 minutes at 4°C in B2G0.5% (50 mM Tris, pH 7, 150 mM NaCl, 5% glycerol, 0.5% Triton-X-100). GST-Cmd1 binding experiments were performed in the absence of exogenous calcium except where indicated. Bound proteins were eluted in sample buffer (50 mM Tris, pH 6.8, 10% glycerol, 10% ß-mercaptoethanol, 2% SDS, 0.1% bromophenol blue) at 100°C. Eluted proteins were separated by SDS-PAGE and visualized by Coomassie blue staining.

Lucifer Yellow Uptake

Yeast cells grown to early-mid logarithmic phase were resuspended in YPD containing 4 mg/mL LY (Invitrogen) and incubated for 1.5-2 hours at 24 or 37°. To stop uptake, 0.4 mL of ice-cold phosphate buffered saline containing 10 mM sodium fluoride and 0.02% sodium azide (PBSNN) was added. To determine vacuolar fluorescence, vacuoles were manually selected in images and total vacuolar fluorescence per cell was calculated using ImageJ software (W.S. Rasband, NIH).

Mup1-GFP Uptake

Yeast cells grown to early-mid logarithmic phase were incubated for 45 minutes at 30°C in the presence or absence of 20 ug/mL methionine. Cells were collected by centrifugation, resuspended in PBSNN and imaged by confocal microscopy. Internal and total fluorescence were determined using ImageJ.

Confocal microscopy

Confocal images were acquired on a Zeiss LSM 5 PASCAL laser-scanning microscope equipped with a Plan-Neofluar 100×/1.45 NA objective (Carl Zeiss MicroImaging, Inc.) using LSM PASCAL software. LY was excited with 458 nm, GFP with 488 nm, and mCherry with 543-nm laser lines. For live cell imaging, yeast strains were grown to 0.2-0.4 OD_{600} in SD medium at room temperature. Cells were collected by centrifugation and resuspended in 0.1 mL of SD, and imaged using spinning disc confocal microscopy at room

temperature. Images were captured on a 3i Marianas SDC confocal microscope equipped with a Zeiss AxioObserver Z1, Yokogawa CSU-22 confocal head and a Hamamatsu EMCCD C9100-13 camera using a 100×/1.45 NA objective. GFP and RFP images were acquired by excitation at 488 nm and 561 nm, respectively. Image acquisition and analysis were performed using Slidebook 4.2 software. Following photobleach correction, the lifetime of an endocytic punctum was measured by calculating the number of positive frames and multiplying by the length of time between frames. Retraction events were calculated by creating a kymograph for each identifiable endocytic event, and counting the number of retractions versus productive endocytic events.

Liposome preparation and liposome binding assays

A synthetic lipid mixture (Wu et al., 2014a) containing 60% DOPC (1,2-dioleoyl-sn-glycero-3-phosphocholine), 20% DOPS (1,2-dioleoyl-sn-glycero-3-phospho-L-serine), 10% DOPE (1,2-dioleoyl-sn-glycero-3-phosphoethanol amine) and 10% PIP_2 (L-α-phosphatidylinositol-4,5-bisphosphate) in chloroform (Avanti Polar Lipids) was dried under a stream of nitrogen, overlaid with argon and stored at −80°C. Lipids were rehydrated in B2 (50 mM Tris, pH 7, 150 mM NaCl) containing 1 mM DTT. Liposomes were extruded 17x through an 800 nm polycarbonate membrane (Whatman) using a Mini-Extruder (Avanti Polar Lipids).

Bacterial lysates containing Rvs167 (1-265)/161 or I138A/Rvs161 dimers in B2G (B2 + 5% glycerol) were incubated with 100-200 ug liposomes for 1 hour on ice. Lysates containing GST±Cmd1 (wild-type or calcium-binding mutants) were added to liposomes and incubated for an additional 1 hour. Sucrose was added to a final concentration of 30% and liposomes were overlaid with 20% sucrose and 5% sucrose. Following centrifugation, liposomes were collected from the interface between 20% and 5% sucrose solutions and solubilized at 100°C in sampl e buffer. Samples were analyzed by SDS-PAGE and Coomassie Blue staining. No difference in Rvs167 (1-265)/161 binding was observed when higher curvature liposomes were prepared by extrusion through a 100nm membrane (data not shown).

Tubulation Assays and Electron Microscopy

Lysates containing Rvs167 (1-265)/161 or I138A/Rvs161 dimers in B2G (~7 ug of each monomer) were incubated with 150 ug yeast liposomes in the absence or presence of purified Cmd1 or Cmd1-6 (35 ug) at room temperature for 30-40 minutes. 5 uL of each sample was applied to Formvar-carbon support film on an electron microscopy grid for 5 minutes at room temperature. Samples were washed twice with B2 containing 0.1% glycerol, and negatively stained with 2% aqueous uranyl acetate for 3 minutes at room temperature, blotted, and allowed to air dry. Samples were imaged using a JEM1200EX transmission electron microscope (JEOL, Japan) using a BioScan600W digital camera (Gatan, U.S.A.). Tubule measurements were performed using ImageJ software. Tubule lengths were calculated by tracing individual tubules from tip to tip or from tip to the intersection with another tubule or liposome. Tubule diameters were calculated by averaging the diameter of three tubule cross sections.

Statistical analysis

Comparisons of means were done by t-test (unpaired or paired, as appropriate) with Bonferroni correction to correct for multiple comparisons. COS7 tubulation experiments were analyzed by logistic regression.

Supplementary Material

Refer to Web version on PubMed Central for supplementary material.

ACKNOWLEDGEMENTS

We would like to thank J. Colicelli, E. Dell'Angelica and A. Munn for critical reading of the manuscript, C. Clarke, K. Cunningham, E. Landaw, and B. Marbois for advice, and D. Cascio for structure prediction. We are grateful to H. Riezman and M. Cyert for yeast strains and antibodies. We thank the Electron Microscopy Laboratory at UCLA. This work was supported by grants from the Jonsson Comprehensive Cancer Center at UCLA and 1F32GM085921 (M.M.) and NIHGM39040 (G.P).

REFERENCES

Artalejo CR, Elhamdani A, Palfrey HC. Calmodulin is the divalent cation receptor for rapid endocytosis, but not exocytosis, in adrenal chromaffin cells. Neuron. 1996; 16:195–205. [PubMed: 8562084]

Bauer F, Urdaci M, Aigle M, Crouzet M. Alteration of a yeast SH3 protein leads to conditional viability with defects in cytoskeletal and budding patterns. Mol Cell Biol. 1993; 13:5070–5084. [PubMed: 8336735]

Berman H, Henrick K, Nakamura H. Announcing the worldwide Protein Data Bank. Nat Struct Biol. 2003; 10:980. [PubMed: 14634627]

Bonilla M, Nastase KK, Cunningham KW. Essential role of calcineurin in response to endoplasmic reticulum stress. Embo J. 2002; 21:2343–2353. [PubMed: 12006487]

Carroll SY, Stirling PC, Stimpson HE, Giesselmann E, Schmitt MJ, Drubin DG. A yeast killer toxin screen provides insights into a/b toxin entry, trafficking, and killing mechanisms. Dev Cell. 2009; 17:552–560. [PubMed: 19853568]

Colwill K, Field D, Moore L, Friesen J, Andrews B. In vivo analysis of the domains of yeast Rvs167p suggests Rvs167p function is mediated through multiple protein interactions. Genetics. 1999; 152:881–893. [PubMed: 10388809]

Cyert MS. Genetic analysis of calmodulin and its targets in Saccharomyces cerevisiae. Annu Rev Genet. 2001; 35:647–672. [PubMed: 11700296]

Daumke O, Roux A, Haucke V. BAR domain scaffolds in dynamin-mediated membrane fission. Cell. 2014; 156:882–892. [PubMed: 24581490]

Drum CL, Yan SZ, Bard J, Shen YQ, Lu D, Soelaiman S, Grabarek Z, Bohm A, Tang WJ. Structural basis for the activation of anthrax adenylyl cyclase exotoxin by calmodulin. Nature. 2002; 415:396–402. [PubMed: 11807546]

Dulic V, Egerton M, Elguindi I, Raths S, Singer B, Riezman H. Yeast endocytosis assays. Methods in Enzymology. 1991; 194:697–709. [PubMed: 2005817]

Friesen H, Humphries C, Ho Y, Schub O, Colwill K, Andrews B. Characterization of the yeast amphiphysins Rvs161p and Rvs167p reveals roles for the Rvs heterodimer in vivo. Mol Biol Cell. 2006; 17:1306–1321. [PubMed: 16394103]

Frost A, Perera R, Roux A, Spasov K, Destaing O, Egelman EH, De Camilli P, Unger VM. Structural basis of membrane invagination by F-BAR domains. Cell. 2008; 132:807–817. [PubMed: 18329367]

Frost A, Unger VM, De Camilli P. The BAR domain superfamily: membrane-molding macromolecules. Cell. 2009; 137:191–196. [PubMed: 19379681]

Geiser JR, van Tuinen D, Brockerhoff SE, Neff MM, Davis TN. Can calmodulin function without binding calcium? Cell. 1991; 65:949–959. [PubMed: 2044154]

Geli MI, Wesp A, Riezman H. Distinct functions of calmodulin are required for the uptake step of receptor-mediated endocytosis in yeast: the type I myosin Myo5p is one of the calmodulin targets. Embo J. 1998; 17:635–647. [PubMed: 9450989]

Grotsch H, Giblin JP, Idrissi FZ, Fernandez-Golbano IM, Collette JR, Newpher TM, Robles V, Lemmon SK, Geli MI. Calmodulin dissociation regulates Myo5 recruitment and function at endocytic sites. Embo J. 2010; 29:2899–2914. [PubMed: 20647997]

Jonsdottir GA, Li R. Dynamics of yeast Myosin I: evidence for a possible role in scission of endocytic vesicles. Curr Biol. 2004; 14:1604–1609. [PubMed: 15341750]

Kaksonen M, Sun Y, Drubin DG. A pathway for association of receptors, adaptors, and actin during endocytic internalization. Cell. 2003; 115:475–487. [PubMed: 14622601]

Kaksonen M, Toret CP, Drubin DG. A modular design for the clathrin- and actin-mediated endocytosis machinery. Cell. 2005; 123:305–320. [PubMed: 16239147]

Kishimoto T, Sun Y, Buser C, Liu J, Michelot A, Drubin DG. Determinants of endocytic membrane geometry, stability, and scission. Proc Natl Acad Sci U S A. 2011; 108:E979–988. [PubMed: 22006337]

Kubler E, Schimmoller F, Riezman H. Calcium-independent calmodulin requirement for endocytosis in yeast. Embo J. 1994; 13:5539–5546. [PubMed: 7988551]

Landt O, Grunert HP, Hahn U. A general method for rapid site-directed mutagenesis using the polymerase chain reaction. Gene. 1990; 96:125–128. [PubMed: 2265750]

Liu Y, Zheng X, Mueller GA, Sobhany M, DeRose EF, Zhang Y, London RE, Birnbaumer L. Crystal structure of calmodulin binding domain of orai1 in complex with Ca2+ calmodulin displays a unique binding mode. J Biol Chem. 2012; 287:43030–43041. [PubMed: 23109337]

Lombardi R, Riezman H. Rvs161p and Rvs167p, the two yeast amphiphysin homologs, function together in vivo. J Biol Chem. 2001; 276:6016–6022. [PubMed: 11096097]

Menant A, Barbey R, Thomas D. Substrate-mediated remodeling of methionine transport by multiple ubiquitin-dependent mechanisms in yeast cells. Embo J. 2006; 25:4436–4447. [PubMed: 16977312]

Miller SE, Mathiasen S, Bright NA, Pierre F, Kelly BT, Kladt N, Schauss A, Merrifield CJ, Stamou D, Honing S, et al. CALM regulates clathrin-coated vesicle size and maturation by directly sensing and driving membrane curvature. Dev Cell. 2015; 33:163–175. [PubMed: 25898166]

Mim C, Cui H, Gawronski-Salerno JA, Frost A, Lyman E, Voth GA, Unger VM. Structural basis of membrane bending by the N-BAR protein endophilin. Cell. 2012; 149:137–145. [PubMed: 22464326]

Mim C, Unger VM. Membrane curvature and its generation by BAR proteins. Trends Biochem Sci. 2012; 37:526–533. [PubMed: 23058040]

Mizuno N, Jao CC, Langen R, Steven AC. Multiple modes of endophilin-mediated conversion of lipid vesicles into coated tubes: implications for synaptic endocytosis. J Biol Chem. 2010; 285:23351–23358. [PubMed: 20484046]

Munn AL, Stevenson BJ, Geli MI, Riezman H. *end5*, *end6*, and *end7*: mutations that cause actin delocalization and block the internalization step of endocytosis in *Saccharomyces cerevisiae*. Molecular Biology of the Cell. 1995; 6:1721–1742. [PubMed: 8590801]

Ohya Y, Botstein D. Diverse essential functions revealed by complementing yeast calmodulin mutants. Science. 1994a; 263:963–966. [PubMed: 8310294]

Ohya Y, Botstein D. Structure-based systematic isolation of conditional-lethal mutations in the single yeast calmodulin gene. Genetics. 1994b; 138:1041–1054. [PubMed: 7896089]

Okano H, Cyert MS, Ohya Y. Importance of phenylalanine residues of yeast calmodulin for target binding and activation. J Biol Chem. 1998; 273:26375–26382. [PubMed: 9756868]

Qualmann B, Koch D, Kessels MM. Let's go bananas: revisiting the endocytic BAR code. Embo J. 2011; 30:3501–3515. [PubMed: 21878992]

Rao Y, Haucke V. Membrane shaping by the Bin/amphiphysin/Rvs (BAR) domain protein superfamily. Cell Mol Life Sci. 2011; 68:3983–3993. [PubMed: 21769645]

Rao Y, Ma Q, Vahedi-Faridi A, Sundborger A, Pechstein A, Puchkov D, Luo L, Shupliakov O, Saenger W, Haucke V. Molecular basis for SH3 domain regulation of F-BAR-mediated membrane deformation. Proc Natl Acad Sci U S A. 2010; 107:8213–8218. [PubMed: 20404169]

Ren G, Vajjhala P, Lee JS, Winsor B, Munn AL. The BAR domain proteins: molding membranes in fission, fusion, and phagy. Microbiol Mol Biol Rev. 2006; 70:37–120. [PubMed: 16524918]

Salisbury JL, Condeelis JS, Satir P. Role of coated vesicles, microfilaments, and calmodulin in receptor-mediated endocytosis by cultured B lymphoblastoid cells. J Cell Biol. 1980; 87:132–141. [PubMed: 6968316]

Schaerer-Brodbeck C, Riezman H. Functional interactions between the p35 subunit of the Arp2/3 complex and calmodulin in yeast. Mol Biol Cell. 2000; 11:1113–1127. [PubMed: 10749918]

Schumacher MA, Rivard AF, Bachinger HP, Adelman JP. Structure of the gating domain of a Ca2+-activated K+ channel complexed with Ca2+/calmodulin. Nature. 2001; 410:1120–1124. [PubMed: 11323678]

Shimada A, Niwa H, Tsujita K, Suetsugu S, Nitta K, Hanawa-Suetsugu K, Akasaka R, Nishino Y, Toyama M, Chen L, et al. Curved EFC/F-BAR-domain dimers are joined end to end into a filament for membrane invagination in endocytosis. Cell. 2007; 129:761–772. [PubMed: 17512409]

Sivadon P, Crouzet M, Aigle M. Functional assessment of the yeast Rvs161 and Rvs167 protein domains. FEBS Lett. 1997; 417:21–27. [PubMed: 9395067]

Sun Y, Martin AC, Drubin DG. Endocytic internalization in budding yeast requires coordinated actin nucleation and myosin motor activity. Dev Cell. 2006; 11:33–46. [PubMed: 16824951]

Vazquez FX, Unger VM, Voth GA. Autoinhibition of endophilin in solution via interdomain interactions. Biophys J. 2013; 104:396–403. [PubMed: 23442861]

Wu T, Shi Z, Baumgart T. Mutations in BIN1 associated with centronuclear myopathy disrupt membrane remodeling by affecting protein density and oligomerization. PLoS One. 2014a; 9:e93060. [PubMed: 24755653]

Wu XS, McNeil BD, Xu J, Fan J, Xue L, Melicoff E, Adachi R, Bai L, Wu LG. Ca(2+) and calmodulin initiate all forms of endocytosis during depolarization at a nerve terminal. Nat Neurosci. 2009; 12:1003–1010. [PubMed: 19633667]

Wu XS, Zhang Z, Zhao WD, Wang D, Luo F, Wu LG. Calcineurin is universally involved in vesicle endocytosis at neuronal and nonneuronal secretory cells. Cell Rep. 2014b; 7:982–988. [PubMed: 24835995]

Yamashita T, Eguchi K, Saitoh N, von Gersdorff H, Takahashi T. Developmental shift to a mechanism of synaptic vesicle endocytosis requiring nanodomain Ca2+ Nat Neurosci. 2010; 13:838–844. [PubMed: 20562869]

Yao L, Sakaba T. Activity-dependent modulation of endocytosis by calmodulin at a large central synapse. Proc Natl Acad Sci U S A. 2012; 109:291–296. [PubMed: 22184217]

Yap KL, Kim J, Truong K, Sherman M, Yuan T, Ikura M. Calmodulin target database. J Struct Funct Genomics. 2000; 1:8–14. [PubMed: 12836676]

Youn JY, Friesen H, Kishimoto T, Henne WM, Kurat CF, Ye W, Ceccarelli DF, Sicheri F, Kohlwein SD, McMahon HT, et al. Dissecting BAR domain function in the yeast Amphiphysins Rvs161 and Rvs167 during endocytosis. Mol Biol Cell. 2010; 21:3054–3069. [PubMed: 20610658]

Zaidel-Bar R, Joyce MJ, Lynch AM, Witte K, Audhya A, Hardin J. The F-BAR domain of SRGP-1 facilitates cell-cell adhesion during C. elegans morphogenesis. J Cell Biol. 2010; 191:761–769. [PubMed: 21059849]

Highlights

- The Rvs167 BAR domain binds calmodulin.
- Calmodulin binding to Rvs167 promotes endocytic vesicle release.
- Calmodulin binding stimulates membrane tubulation and constriction by Rvs167.
- Calmodulin can stimulate tubulation by endophilin A2 BAR domain in mammalian cells.

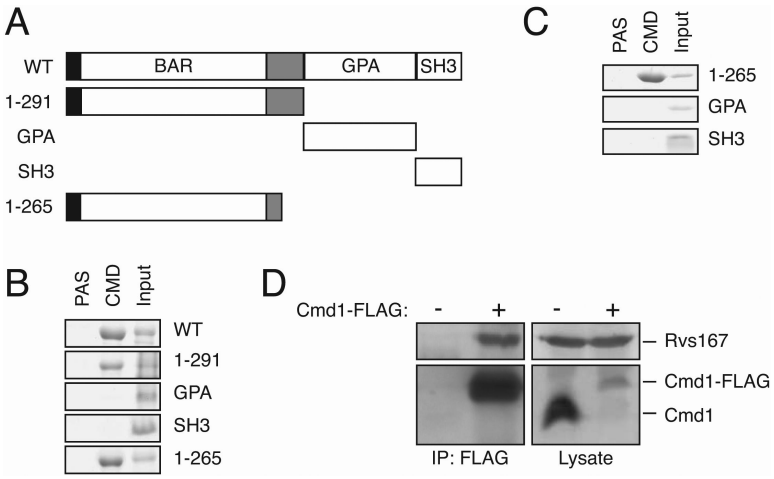

Figure 1. Rvs167 N-BAR domain binds calmodulin

(A) Diagram of Rvs167 fragments. The black box represents the N-terminal amphipathic helix. The grey box represents a spacer region. (B) Rvs167 binds calmodulin. The indicated Rvs167 fragments in bacterial lysates (Input = 5%) were tested for binding to calmodulin-Agarose (CMD) or protein A sepharose (PAS). Proteins separated by SDS-PAGE were visualized with Coomassie blue. (C) Rvs167 1-265 binds directly to calmodulin. The indicated purified Rvs167 fragments (Input = 3%) were tested for binding to CMD. Proteins were analyzed as in (B). (D) Rvs167 binds Cmd1 *in vivo*. Yeast cell extracts (Lysate = 2%) expressing calmodulin with (+) or without (−) a FLAG tag were subjected to immunoprecipitation with anti-FLAG antibodies. Immunoprecipitated proteins were separated by SDS-PAGE and visualized by immunoblotting for Rvs167 or Cmd1.

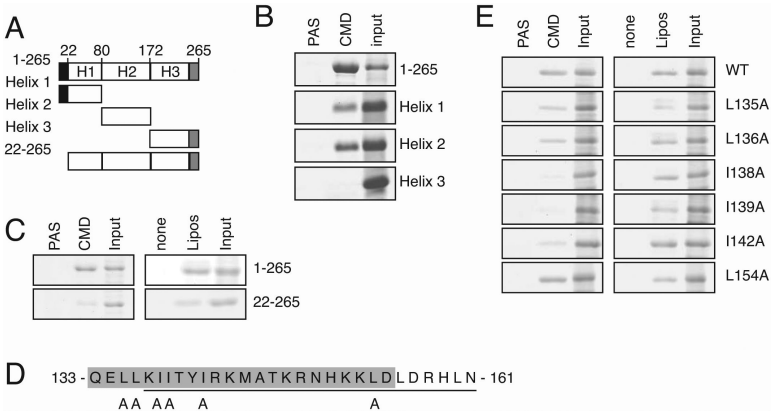

Figure 2. Rvs167 N-BAR domain contains two calmodulin binding regions

(A) Diagram of Rvs167 fragments. (B) Helices 1 and 2 of Rvs167 bind calmodulin. The indicated Rvs167 fragments in bacterial cell lysates were tested for binding to CMD or PAS (input = 3%) as in Figure 1B. (C) Optimal 1-265 binding to both calmodulin and liposomes requires the N-terminal amphipathic helix. The indicated Rvs167 fragments in bacterial lysates were tested for binding to CMD (input = 2%) or liposomes (input = 10%). Proteins were analyzed as in Figure 1B. (D) Potential calmodulin binding region in helix 2. Sequence predicted to bind calmodulin by the Calmodulin Target Database is highlighted in grey. Underlined region is required for calmodulin binding in vitro. Also see Figure S1. Alanine mutations used in this study are indicated. (E) Mutations of hydrophobic residues in the helix 2 binding region decrease binding to calmodulin. The indicated Rvs167 mutants (in 1-265) from bacterial lysates (input = 20%) were tested for calmodulin or liposome binding as in (C).

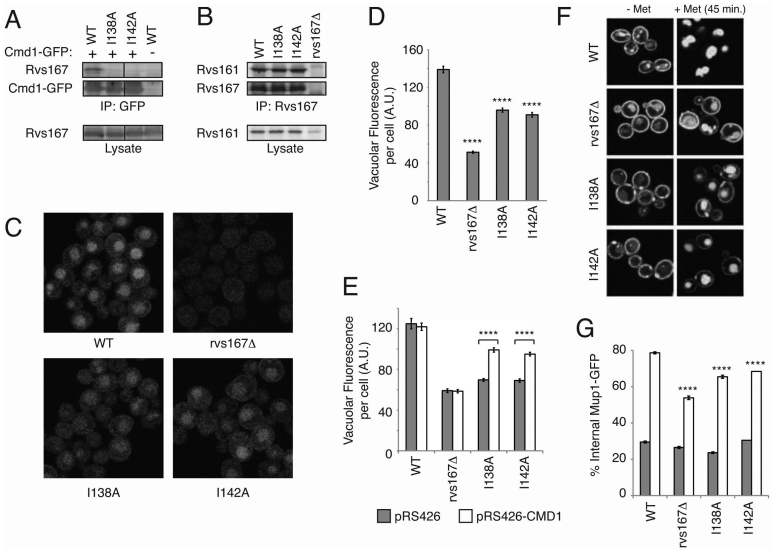

Figure 3. Calmodulin binding mutants of Rvs167 are defective in endocytosis

(A) Rvs167 mutants are defective in calmodulin binding *in vivo*. Lysates (1%) from wild-type (WT) or indicated Rvs167 mutant yeast cells expressing Cmd1-GFP (+) or untagged Cmd1 (−) were subjected to immunoprecipitation with anti-GFP antibodies. Immunoprecipitated proteins were separated by SDS-PAGE and visualized by immunoblotting for Rvs167 or GFP. (B) Rvs167 mutants bind Rvs161. Lysates (1%) from WT or indicated Rvs167 mutant yeast cells were subjected to immunoprecipitation with anti-Rvs167 antibodies. Immunoprecipitated proteins were separated by SDS-PAGE and visualized by immunoblotting for Rvs161 or Rvs167. As previously reported (Lombardi and Riezman, 2001), expression of Rvs161 is decreased in *rvs167*Δ cells. (C) Calmodulin binding mutants of Rvs167 are defective in LY endocytosis. The indicated strains were assessed for LY internalization by confocal microscopy. (D) Quantitation of vacuolar LY in strains presented in (C). Bars indicate the mean total vacuolar fluorescence per cell ± s.e.m. in arbitrary units (A.U.). **** $p < 0.0001$ compared to WT as determined by t-test. (E) Calmodulin overexpression partially rescues LY endocytosis in I138A and I142A mutant cells. The indicated strains expressing CMD1 from a multicopy vector (pRS426-CMD1) or vector alone (pRS426) were tested for LY uptake and the results quantified as in (D). **** $p < 0.0001$ as compared to empty vector as determined by t-test for each strain. Also see Figure S2. (F) Impaired Mup1-GFP endocytosis in Rvs167 mutants. Endocytosis of Mup1-GFP in the indicated strains was monitored by confocal microscopy 45 minutes after incubation in the presence (+Met) or absence of methionine (−Met). (G) Quantitation of Mup1-GFP internalization in strains presented in (F). Mup1-GFP internalization was quantified in the absence of methionine (closed bars) and 45 minutes after methionine addition (open bars) by determining the percentage of internalized Mup1-GFP signal as compared to total cell fluorescence. Bars show the mean ± s.e.m. of multiple independent transformants. **** $p < 0.0001$ compared to WT as determined by t-test.

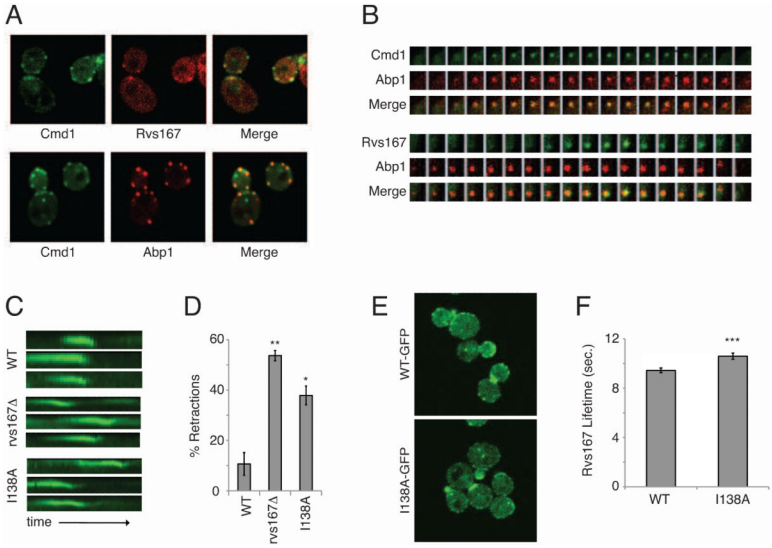

Figure 4. Defective endocytic vesicle formation in Rvs167 calmodulin-binding mutants

(A) Cmd1 colocalizes with Rvs167 and Abp1 at sites of endocytosis. Yeast expressing Cmd1-GFP and either Rvs167-2XRFP or Abp1-RFP were visualized using spinning disc confocal microscopy. (B) Cmd1 localizes to sites of endocytosis with dynamics similar to Abp1. Yeast co-expressing Abp1-RFP with either Cmd1-GFP or Rvs167-GFP were imaged over time by spinning disc confocal microscopy. Images show consecutive frames from movies of representative endocytic events. Each frame represents 1 second. (C) Rvs167 mutants display increased Sla1 retractions. Sla1-GFP in WT, *rvs167*Δ and I138A mutant cells was imaged using spinning disc confocal microscopy. Kymographs show representative retraction events in mutant cells. (D) Quantitation of retraction events. Mean percentage retraction events ± s.e.m. was determined by analyzing endocytic events in WT, *rvs167*Δ and I138A mutants for three independent experiments. ** and * $p < 0.01$ or 0.05 compared to WT, respectively, as determined by t-test. (E) Rvs167 localizes to endocytic sites normally in I138A mutant cells. Yeast strains expressing Rvs167-GFP or I138A-GFP were imaged by confocal microscopy. (F) Rvs167-GFP lifetime is slightly longer in I138A mutant cells. Mean lifetimes of Rvs167-GFP ± s.e.m. were calculated from images acquired by spinning disc confocal microscopy. *** $p< 0.001$ as compared to WT as determined by t-test.

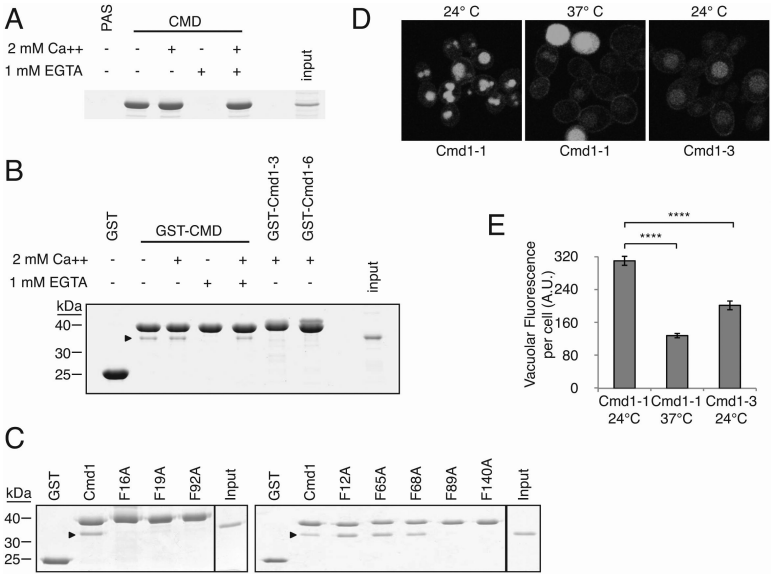

Figure 5. Calcium is required for calmodulin-Rvs167 binding and optimal endocytosis

(A,B) Rvs167 binding to calmodulin requires calcium. Rvs167 aa1-265 in bacterial lysate (Input = 2.5%) was tested for binding to calmodulin-agarose (A) or GST, GST-Cmd1, GST-Cmd1-3 and GST-Cmd1-6 (B) in the absence or presence of $CaCl_2$ and/or EGTA. Bound proteins were separated and detected by Coomassie blue as in Figure 1B. Arrowhead in (B) indicates Rvs167 aa1-265. (C) Calmodulin residues required for endocytosis are also required for Rvs167 binding. Purified Rvs167 aa1-265 (Input = 4%) was tested for binding to GST, GST-Cmd1 or the indicated mutant forms of GST-Cmd1 immobilized on glutathione-sepharose. Bound proteins were analyzed as in (A). Arrowhead indicates bound Rvs167 aa1-265. (D) Calcium binding by Cmd1 is required for optimal LY endocytosis. LY uptake was assessed by confocal microscopy in cells expressing the calcium-binding calmodulin mutant *cmd1-3* or the temperature-sensitive calmodulin mutant *cmd1-1* at the indicated temperatures. Cell death accounts for the bright, fully-stained *cmd1-1* cells at 37°C. Also see Figure S3. (E) Quantitatio n of vacuolar LY in *cmd1-1* or *cmd1-3* in strains presented in (D). **** $p < 0.0001$ as determined by t-test.

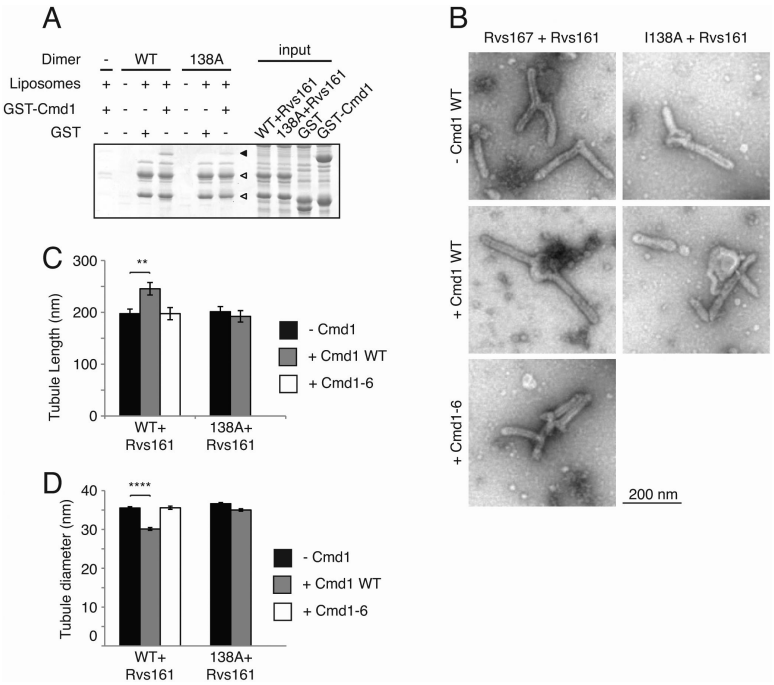

Figure 6. Calmodulin lengthens and constricts tubules generated by Rvs167

(A) Calmodulin does not affect binding of Rvs167/161 to liposomes. Rvs167 1-265 or I138A Rvs167 1-265 was co-expressed with Rvs161 in bacteria and tested for liposome binding in the presence of GST or GST-Cmd1. Liposome-bound proteins were analyzed as in Figure 2C. Also see Figure S4A. Closed arrowhead indicates GST-Cmd1. Open arrowheads indicate Rvs167 (1-265) and Rvs161. (B) Calmodulin enhances tubulation by Rvs167 (1-265)/161. Liposomes incubated with Rvs167 (1-265)/161 (left column) or I138A/Rvs161 (right column) in the absence (top row) or presence of calmodulin (middle row) or Cmd1-6 (bottom row) were analyzed by electron microscopy. See also Figure S4B,C. (C,D) Tubule lengths (C) and diameters (D) generated by Rvs167 (1-265)/161 or I138A/Rvs161 in the absence (−Cmd1) or in the presence of wild-type calmodulin (+Cmd1) or Cmd1-6. Bars in (C) and (D) show the mean tubule length or diameter ± s.e.m. ** and **** $p < 0.01$ or 0.0001 compared to Rvs167 (1-265)/161 without calmodulin as determined by t-test. Also see Figure S4D,E.

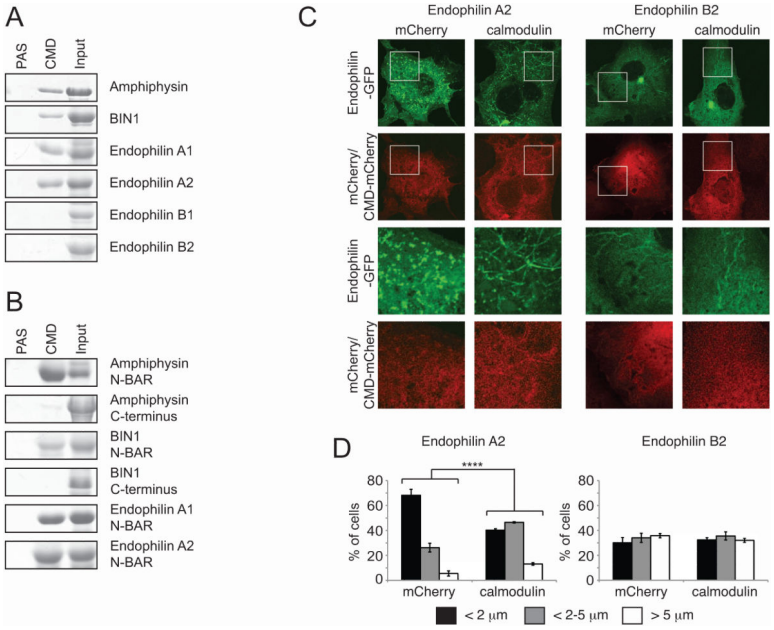

Figure 7. A subset of mammalian N-BAR domains are regulated by calmodulin

(A) Amphiphysin, BIN1 and endophilins A1 and A2 bind calmodulin. The indicated N-BAR domain proteins in bacterial lysates (Input = 2.5%) were tested for binding to CMD or PAS as in Figure 1B. (B) Mammalian N-BAR domains bind calmodulin. The N-BAR domain or C-terminal regions of the indicated proteins in bacterial lysates (Input = 2.5%) were tested for binding to CMD as in (A). (C) Co-expression of calmodulin with endophilin A2 promotes tubulation *in vivo*. Endophilin A2-GFP or endophilin B2-GFP was co-expressed with mCherry or calmodulin-mCherry in COS7 cells. Cells were imaged by confocal microscopy. Arrowheads indicate examples of tubules labeling with both endophilin A2 and calmodulin. Scale bar = 10 μm. Lower two rows display enlargements of boxed areas in upper two rows. Also see Figure S5. (D) Quantitation of tubulation in cells expressing endophilin A2-GFP or endophilin B2-GFP without (mCherry) or with calmodulin-mCherry (calmodulin). For each population, the percentage of cells exhibiting GFP-labeled tubules that were predominantly <2 μm, 2-5 μm, or >5 μm was determined for three independent experiments ± s.e.m. **** $p < 0.0001$ as determined by logistic regression.